International Conference on Renewable Energies and Power Quality (ICREPQ'19)
Tenerife (Spain), 10th to 12th April, 2019
Renewable Energy and Power Quality Journal (RE&PQJ)
ISSN 2172-038 X, No.17 July 2019

Heat treatment of iron/carbon composites for energy storage: effect on physicochemical and electrochemical properties

J. R. F. Gonçalves[1], C.F. Malfatti[1], E. Leal da Silva[1,2], G.R. Gonçalves[3], Miguel A. Schettino Jr.[3], Jair C. C. Freitas[3], and A. Cuña[2]

[1] LAPEC/PPGE3M, Universidade Federal do Rio Grande do Sul, Av. Bento Gonçalves, 9500, setor 4, prédio 43427, sala 232 - 91501-970 – Porto Alegre/RS (Brazil)
Phone/Fax number: +55 51 33089405, e-mail: jorgerafael.uergs@gmail.com, celia.malfatti@ufrgs.br
[2] Area Fisicoquímica, DETEMA, Facultad de Química, Universidad de la República, Montevideo 11800 (Uruguay)
Phone/Fax number: +598 29248352, e-mail: elenleal@fq.edu.uy, acuna@fq.edu.uy
[3] Laboratory of Carbon and Ceramic Materials, Department of Physics, Federal University of Espírito Santo, Av. Fernando Ferrari, 514, Goiabeiras, 29075-910 - Vitória, ES, Brazil. E-mail: jairccfreitas@yahoo.com.br

Abstract. Carbon materials are widely used as supercapacitor electrodes while iron oxides and other iron compounds are promising electrode materials due to its pseudocapacitive contribution. This work deals with the preparation and electrochemical characterization of iron/carbon composites for supercapacitor electrode applications. The carbon precursor samples were prepared from a carbonization of babassu coconut endocarp, and the iron/carbon nanocomposites were obtained by precipitation synthesis using iron salt, followed by a heat treatment at different temperatures. The electrochemical characterization of the samples show that, at low current density, the sample without iron compounds shows the higher electrical capacitance, up to 98 F g^{-1} in 2 M H_2SO_4. This good performance can be associated to a pseudocapacitive contribution of the oxygenated functional groups present in this sample. However, at higher current densities, the best electrochemical behaviour was achieved for the sample treated at 1000 °C. This good performance is may be associated to the Fe^o and Fe_3C nanoparticles present in the sample which can enhance its electrical conductivity. On the other hand, is no there clearly evidence of pseudocapacitive contribution of the iron particles. Future works will seek to improve the surface area of the materials with the aim to increase the double layer capacitance, and also to perform electrochemical studies using other electrolytes.

Key words

Energy storage, Supercapacitors, Pseudocapacitance, iron compounds, Biomass carbon materials

1. Introduction

The sustainable and intelligent use of energy necessarily implies the use of different energy storage devices [1]. In recent years, electrochemical capacitors, also known as supercapacitors (SCs), have received great scientific and technological attention because of their interesting possibilities in this field [2, 3]. Although different commercial devices already exist, there are still many scientific and technological challenges in supercapacitors research area. One of the main current challenges is to increasing the amount of the stored energy. This can be achieved through the development of suitable, low-cost and environmentally friendly electrode materials [3].

Activated carbon materials (aCMs) are one of the most studied and used SCs electrode materials. They can have high specific electrical capacitance (mainly due to their large specific surface area) and electrical conductivity, good electrochemical stability and moderate cost [4, 5]. Besides, surface nitrogenated and/or oxygenated functional groups in aCMs can increase the observed electrical capacitance through reversible redox reactions (faradaic contribution), a phenomenon usually called pseudocapacitance [6, 7, 8]. An important group of aCMs, suitable for SC electrode application, are those that can be obtained from lignocellulosic precursors [5, 9, 10, 11], which have the important advantage that can be prepared from abundant, renewable and cheap natural resources. In recent years, several examples of lignocellulosic residues have been successfully used for aCMs preparation, including rice hulls, sugarcane bagasse, coconut, among many others [5, 12]. The endocarp of babassu coconut (here named as EB) constitute an example of an abundant lignocellulosic residue, generated in large amounts in Brazil [13], which has found promising applications as a chars precursor, of porous carbons and nanocomposites materials [14, 15, 16]. On the other hand, iron materials (e.g., Fe_2O_3, FeOOH) have been studied as pseudocapacitive materials showing interesting characteristics for SC electrode application. The use of iron-based materials as SC electrodes has some important advantages since Fe-containing precursors are abundant, environmentally

friendly and have low cost. Besides, Fe/carbon nanocomposites have better electrochemical performance compared to Fe-containing compounds due to the synergy between the carbon support and the pseudocapacitive iron compounds [17, 18].

In this work, we present the study of the electrochemical behavior as SC material of nanocomposite iron oxide /EB. The nanocomposites were prepared following the precipitation method using a commercial iron salt and an aCM obtained from EB_OxFe, with a subsequent thermal treatment at 1000 °C. The electrochemical analysis of the samples includes charge-discharge curves and cyclic voltammetry and electrochemical impedance, using aqueous sulfuric acid solution as electrolyte. The electrochemical results were correlated with the physicochemical characterization of the samples.

2. Materials and methods

A. Materials synthesis

The biomass derived carbon used as support of the Fe-containing compounds was obtained by carbonization of EB at 700 ºC, for 1 h in a tubular furnace under N_2 flow. The obtained sample (EBC) was washed with abundant distilled water until reaching a nearly neutral pH, vacuum filtered and finally dried at 110 ºC. The iron/carbon nanocomposites were prepared by a simple precipitation method, using iron nitrate ($Fe(NO_3)_3 \cdot 9H_2O$, from Vetec) as the iron source and ammonium hydroxide (NH_4OH, from Merck) as the precipitating agent. The synthesis was conducted by mixing 105.3 g of EBC with 57.7 g of $Fe(NO_3)_3 \cdot 9H_2O$ in 250 mL of distilled water, followed by the gradual addition (at a rate of ca. 10 mL min^{-1}) of an aqueous solution of NH_4OH (1.4 mol L^{-1}) and stirring for 24 h at room temperature, resulting in a gel-like product. This material was repeatedly washed with distilled water until reaching a nearly neutral pH, vacuum filtered and dried at 110 ºC for 2 h; the obtained product was named EBC_OxFe. Next, this material was heat-treated under N_2 gas flow, using a tubular furnace at a heating-rate of 5 °C min^{-1} up to temperatures in the range 700-1000 ºC and with a residence time of 2 h at each final temperature. The products obtained after each heat treatment were named EBC_OxFe_XX samples, where XX represents the heat treatment temperature, in ºC.

B. Physicochemical characterization

The elemental analysis (C, H, N and O contents) was conducted using a Leco CHNS932 instrument coupled to a VTF900 furnace. Fe contents were determined by X-ray fluorescence, using a Shimadzu EDX700 spectrometer Ash content was quantified as the remaining mass in a thermogravimetric analysis (TGA) in ar atmosphere. TGA was carried out in a TA INSTRUMENTS, model Q600, equipment, with a heating rate of 10 ° min^{-1} from room temperature to 900 ºC.

X-ray diffraction (XRD) patterns were recorded at room temperature in a Shimadzu XRD-6000 powder diffractometer with Cu-Kα radiation (λ = 1.5418 Å); the diffraction angle (2θ) was varied from 10 to 90° at steps of 0.02°. Textural analysis was conducted by recording N_2 adsorption/desorption isotherms at 77 K, using a Quantachrome Autosorb-1 instrument. The specific surface area (SSA) values were determined by the Brunauer, Emmett and Teller (BET) method.

C. Electrochemical characterization

The samples were electrochemically characterized by galvanostatic charge/discharge curves, cyclic voltammetry and electrochemical impedance spectroscopy (EIS) experiments. These experiments were carried out in a three electrode cell using a 2 mol L^{-1} H_2SO_4 aqueous solution electrolyte. As working electrode, a suspension of about ~1.4 mg of the analyzed sample in Nafion® (5 wt%) was coated onto a graphite disk with geometric area of 0.29 cm^2. Platinum wire and Ag/AgCl (satured in KCl) were used as counter and potential reference electrodes, respectively. The gravimetric specific capacitance (C_s) expressed in F g^{-1} was determined from galvanostatic charge/discharge curves in the voltage range of 0 to 0.8 V *vs.* Ag/AgCl, at current range of 3 to 30 mA. C_s was determined at each current according to the following equation: $C = I \cdot t_d / E_2 \cdot m_e$ where I is the constant applied current in amperes, t_d is the discharge time in seconds, E_2 is the voltage range during the discharge in volts, and m_e is the mass of the analyzed sample in the working electrode expressed in grams. Cyclic voltammograms were obtained in the potential window of -0.2 V to 0.8 V *vs.* Ag/AgCl at scan rate of 50 mV s^{-1}. All the experiments were performed at room temperature with a PGSTAT 302N Autolab potentiostat/galvanostat/FRA.

3. Results and discussion

A. Physicochemical results

The values of the elemental analysis, ash content and iron content are shown in Table I. The analysed samples present higher carbon content, above 70%, with a low hydrogen and nitrogen content (around 1%), which expected for a biomass derived carbon material. The EBC sample also contains oxygen and nitrogen (10.5% and 0.9 % respectively) those that are part of the different oxygenated and nitrogenated functional groups of the sample. The carbon content of the EBC_OxFe (71 %), sample is lower than the EBC which can be explained by the higher presence of the iron particles, causing an increase in ash, oxygen and iron content (see Table I).

Table I. - Elemental analysis of the samples

Sample	**C %**	**H %**	**N %**	**O %**	**Ash* %**	**Fe %**
EBC	81	0.6	0.9	10.5	4.4	0.2
EBC_OxFe	71	1.0	0.9	13.5	10.3	7.0
EBC_OxFe700	77	0.7	1.0	9.8	9.9	7.5
EBC_OxFe900	81	0.4	0.6	3.9	12.4	7.9
EBC_OxFe1000	78	0.3	0.5	5.2	12.5	8.0

Note: * In Fe-containing samples, the ash content of EBC sample has been subtracted.

Considering that the ash content for the Fe-containing samples was determined by subtracting the ash content of the precursor material (EBC), the ash content shown in Table I for the Fe-containing samples corresponds to the Fe compounds present in these samples. After the heat treatment, the ash and Fe content slightly increases with values close to 12% and 7-8% respectively. The heat treatment of the samples also determines a decrease in the oxygen content, and taking into account that the content of iron particles did not change appreciably, this suggests that the iron particles present in the no-treated sample have been transformed to other iron phases. The different iron phases present in the samples (determined by DRX analysis) are shown in the Table II. In the sample EBC_OxFe, no XRD peaks were observed (not shown here) which suggest that there is no formation of iron crystalline phases. Thus, this sample may contain amorphous Fe_3O_4. After the heat treatment, different iron phases (α-Fe, γ-Fe (C), Fe_3C) are formed. The estimation of crystallite size for these phases indicates that the nanoparticles present in the samples would have a particle size about 15-30.

With respect to the textural properties of the samples, it can be seen that the surface area values of all the samples are very similar, around 300 to 400 $m^2\ g^{-1}$. These values can be considered as average values (neither too high nor too low) according to what is expected for a no activated carbon material [19]. According to the pore size distribution (not showed here), the analyzed materials are mainly microporous (pore size below 2 nm) with very little porosity mesoporosity (above 2 nm).

Table II. - Phases present in the samples, BET specific surface area and capacitance values of the samples

Sample	**Phases***	**S_{BET} $m^2\ g^1$**	**C_{dl} F g^{-1}**	**C_3 Fg^{-1}**	C_{30} Fg^{-1}
EBC	C (Turb)	393	39	98	8
EBC_OxFe	Fe^{3+} oxides	352	35	6	1
EBC_OxFe700	Fe_3O_4	362	36	76	6
EBC_OxFe900	Fe_3O_4; α-Fe; Fe_3C; γ-Fe(C)	430	43	49	23
EBC_OxFe1000	Fe_3C; α-Fe; γ-Fe(C)	312	31	56	34

Note: *Determined by DRX. C_{dl} = expected double layer capacitance according to the S_{BET}. C_3 and C_{30} is the observed capacitance at 3 and 30 mA respectively.

B. Electrochemical characterization

Fig. 1 shows the graph of electric capacitance vs. current density, obtained from the galvanostatic curves in 2M H_2SO_4 electrolyte. In order to analyze this graph we have divide it into two zones, a zone with low current density (j <10 A g^{-1}) and a zone with high current density (j> 10 A g^{-1}).

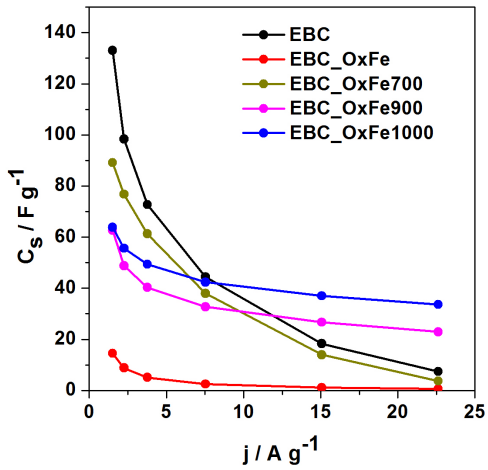

Figure 1. Electric capacitance vs. current density obtained for the different samples.

At low current densities, higher capacitance is observed for the EBC sample, which may be related to a pseudocapacitance contribution of the oxygenated or nitrogenated functional groups present in this sample [2, 8, 19]. The presence of these reversible redox reactions can be evidenced in the voltammograms of Fig. 2. In the EBC sample curve, a broad peak between + 0.3 and + 0.7 V *vs.* Ag/AgCl is clearly observed, indicating the presence of the above mentioned electrochemical reactions. The oxygenated functional groups can also determine a higher capacitance of the EBC sample due to a better wettability of the electrode surface, facilitating the arrival of the electrolyte on whole surface of the material [2, 8, 19]. This would determine a larger "available" surface area for the double layer formation. According to these results, the pseudocapacitance contribution of the iron particles in the treated materials would not be as important as the above discussion about the positive contribution of the oxygenated functional groups present in the EBC sample.

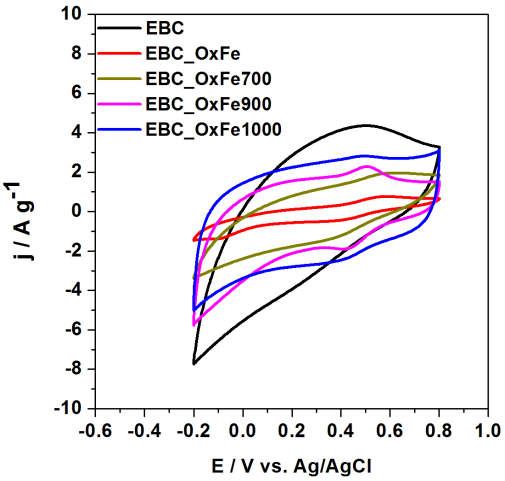

Figure 2. Cyclic voltammograms obtained for the different sample at 50 mV s^{-1} in potential windows of -0.2 V to 0.8 V *vs.* Ag/AgCl.

Continuing with the analysis of the Fig. 1, a capacitance drop is observed for all samples. When the heat treatment

temperature increases (from 700 to 900 and 1000 ° C), the capacitance drop is less pronounced than was observed for the EBC and EBC_OxFe700 samples. This may be related to the higher electrical conductivity of the heat treated samples. On the other hand, for the samples treated at higher temperature, the formation of metal Fe^o and Fe_3C phases would increase the conductivity since these phases have high intrinsic electrical conductivity. The difference in electrical conductivity can also be evidenced in the voltammograms of Fig. 2. The voltammograms obtained for the EBC_OxFe900 and EBC_OxFe1000 samples show a more vertical current rise at the beginning of the anodic scan while the EBC, EBC_OxFe and EBC_OxFe700 samples show a less pronounced current rise. It is well known that the slope of the current rise at the beginning of the anodic scan is inversely proportional to the electrochemical resistance of the cell [2]. Besides, this resistance can be also associated with the electrical resistance of the electrode material. In order to quantify the pseudo-capacitive contribution of the samples, the expected specific double layer capacitance of the samples is determined considering the S_{BET} values. For carbon materials such as those used in this work, using H_2SO_4 aqueous solution electrolyte, the double layer capacitance (C_{DL}) value can be considered equal to 0.10 F m^{-2} [2, 20] and the C_{DL} can be determined by the following equation:

$$C_{DL} = 0.10 \text{ F m}^{-2} \text{ x } S_{BET} (\text{m}^2 \text{ g}^{-1}) \quad (1)$$

Table II shows C_{DL} values for each sample, determined from the equation 1. These C_{DL} values can be compared with the capacitance values obtained at low and high current density. In all samples, except the EBC_OxFe sample, the capacitance values at low current are higher than the calculated C_{DL}, so, it can be concluded that these samples present a pseudocapacitive component in the total their total observed capacitance. For higher current densities, a drop in the capacitance values is observed, an can be explained taking into account that in high currents, there is not enough time to the pseudocapacitance reactions occurs. On the other hand, the double layer capacitance (ideally does not involve the exchange of electrons or atoms) should not be very affected by the increase in current density. This last behaviour was observed for the EBC_OxFe900 and EBC_OxFe1000 samples, while in the case of the EBC, EBC_OxFe and EBC_OxFe700 samples, the capacitance is even lower than the expected for the double layer. As was mentioned above, this important decrease can be related to the low electrical conductivity of these materials.

Comparing the capacitance values obtained for the studied materials with others reported in the literature, the materials obtained in this work have lower capacitance than other similar carbon materials which can reach capacitance up to 200-250 F g^{-1} [2, 19]. However, considering the obtained results, it can be seen an improvement of the electrical and electrochemical properties of the iron/carbon material due to the heat treatment performed at high temperatures. In the case of the EBC_OxFe sample, it capacitance was very low, even at low current density. This behaviour can be explained if it is considered that the amorphous Fe_3O_4 compound present in this sample may be blocking the pores of the carbon material, leaving a little available surface area for the double layer formation. Besides, the iron phase can determines a low electrical conductivity of the sample, permit a polarization of the entire surface of the electrode material.

4. Conclusion

All the prepared carbon based materials have similar specific surface area with pore size in the range of micropores. The EBC_OxFe sample contains amorphous iron phase and the subsequent thermal treatment allow producing an iron/carbon compound with the presence of different iron phases according to the temperature of the heat treatment. At low current density, the sample EBC show the higher electrical capacitance (up to 98 F g^{-1}) that may be related to the oxygenated functional groups which can contribute to the total capacitance through pseudocapacitive reactions. On the other hand, at higher current densities, the best behaviour was achieved for the sample treated at 1000 °C. This good performance is may be associated to the Fe^o and Fe_3C nanoparticles present in the sample which can enhance the electrical conductivity of the sample. On the other hand, is no there clearly evidence of pseudocapacitive contribution of the iron particles. Future works will seek to improve the surface area of the materials with the aim to increase C_{DL}, and also to perform electrochemical studies using basic and neutral aqueous electrolytes.

Acknowledgement

E. Leal da Silva thanks the Uruguayan Comisión Académica de Posgrado (CAP-Udelar) for the Postdoctoral Fellowship (2018-2020). J. C. C. Freitas, G. R. Gonçalves and M. A. Schettino Jr. acknowledge the support from the Brazilian agencies CNPq (grant 408001/2016-0), FAPES (grant 73296872, TO 21/2016).

References

[1] REN21. 2013. Renewables Global Futures Report (Paris: REN21)

[2] Béguin F, Frąckowiak E. Supercapacitors: Materials, Systems, and Applications. Wiley-VCH Verlag GmbH & Co. Weinheim, 2013.

[3] A. González, E. Goikolea, J.A. Barrena, R. Mysyk, Review on supercapacitors: Technologies and materials, Renew Sust Energ Rev 2016, Vol. 58, pp. 1189–1206.

[4] G. Wang, L. Zhang, J. Zhang, A review of electrode materials for electrochemical supercapacitors, Chem. Soc. Rev. 2012, Vol. 41, pp. 797-828.

[5] D. Liu, S. Yu, Y. Shen, H. Chen, Z. Shen, S. Zhao, S. Fu, Y. Yu, B. Bao, Polyaniline Coated Boron Doped Biomass Derived Porous Carbon Composites for Supercapacitor Electrode Materials, Ind. Eng. Chem. Res. 2015, Vol. 54, pp. 12570-12579.

[6] C. Breitkopf, K. Swider-Lyons, Handbook of Electrochemical Energy, Springer-Verlag Berlin Heidelberg, 2017.

[7] B.E. Conway, Electrochemical supercapacitors, Scientific Fundamentals and Technological applications. Kluwer Academic/Plenum Publishers, New York, 1999.

[8] A.G. Pandolfo, A.F. Hollenkamp, Carbon properties and their role in supercapacitors, J. Power Sources 2006, Vol. 157, pp. 11-27.
[9] A. Cuña A, N. Tancredi, J. Bussi, A. C. Deiana, M. F. Sardella, V. Barranco, J. M. Rojo, E. grandis as a biocarbons precursor for supercapacitor electrode application, Waste and Biomass Valor. 2014, Vol. 5, pp. 305-313.
[10] A. Cuña, M. R. Ortega Vega, E. Leal da Silva, N. Tancredi, C. Radtke, C. F. Malfatti, Nitric acid functionalization of carbon monoliths for supercapacitors: Effect on the electrochemical properties, Int. J. Hydrogen Energy 2016, Vol. 41, pp. 12127-12135.
[11] A. Cuña, N. Tancredi, J. Bussi, V. Barranco, T. A. Centeno, A. Quevedo, J. M. Rojo, Biocarbon Monoliths as Supercapacitor Electrodes: Influence of Wood Anisotropy on Their Electrical and Electrochemical Properties, J. Electrochem. Soc. 2014, Vol.161, pp. A1806- A1811.
[12] Z. Gao, Y. Zhang, N. Song, X. Li, Biomass-derived renewable carbon materials for electrochemical energy storage, Mater. Res. Lett. 5 (2017) 89-98.
[13] M.A. Teixeira, Babassu – A new approach for an ancient Brazilian biomass, Biomass Bioenerg. 32 (2008) 857-864.
[14] F.G. Emmerich, C. A. Luengo, Babassu charcoal: a sulfurless renewable thermo-reducing feedstock for steelmaking, Biomass Bioenerg 1996, Vol. 10, pp. 41-44.
[15] G.R. Gonçalves, M.A. Schettino Jr., M.K. Morigaki, E. Nunes, A.G. Cunha, F.G. Emmerich, E.C. Passamani, E. Baggio-Saitovitch, J.C.C. Freitas, Synthesis of nanostructured iron oxides dispersed in carbon materials and in situ XRD study of the changes caused by thermal treatment, J. Nanopart. Res. 2015, Vol. 17, pp. 303-313.
[16] T.R. Lopes, D.F. Cipriano, G.R. Gonçalves, H.A. Honorato, M.A. Schettino Jr., A.G. Cunha, F.G. Emmerich, J.C.C. Freitas, Multinuclear magnetic resonance study on the occurrence of phosphorus in activated carbons prepared by chemical activation of lignocellulosic residues from the babassu production. J. Chem. Environ. Eng. 2017, Vol. 5, pp. 6016-6029.
[17] J. Sun, P. Zan, X. Yang, L. Ye, L. Zhao, Room-temperature synthesis of Fe_3O_4/Fe-carbon nanocomposites with Fe-carbon double conductive network as supercapacitor, Electrochim. Acta 2016, Vol. 215, pp. 483-491.
[18] Y. Li, Q. Li, L. Cao , X. Cui , Y. Yang, P. Xiao, Y. Zhangb, The impact of morphologies and electrolyte solutions on the supercapacitive behavior for Fe_2O_3 and the charge storage mechanism, Electrochim. Acta 2015, Vol. 178, pp. 171-178.
[19] M. INAGAKI *et al.* Advanced Materials Science and Engineering of Carbon. 1st ed. New York: Elsevier; 2014.
[20] PATRICE S.; GOGOTSI Y. Materials for electrochemical capacitors. Mature Materiais, 2008, Vol. 7, pp. 845 – 854.